END
DATE
FILMED
2-84
DTIC

1.0

1.1

1.25 1.4 1.6

4.5
5.0
5.6

2.8 2.5

3.2 2.2

3.6

4.0 2.0

1.8

MICROCOPY RESOLUTION TEST CHART
NATIONAL BUREAU OF STANDARDS-1963-A

LEVEL

OPTICAL EXCITATION OF MOS INTERFACE STATES

Final Technical Report

by

M. Schulz and K. Blumenstock

October 1980

EUROPEAN RESEARCH OFFICE

United States Army

London   England

GRANT NUMBER DAJA 37-79-C-0547

Institut für Angewandte Physik

Universität Erlangen-Nürnberg

81 1 23 051

REPORT DOCUMENTATION PAGE		READ INSTRUCTIONS BEFORE COMPLETING FORM
1. REPORT NUMBER	2. GOVT ACCESSION NO. AD-A094 080	3. RECIPIENT'S CATALOG NUMBER
4. TITLE (and Subtitle) Optical Excitation of MOS Interface States		5. TYPE OF REPORT & PERIOD COVERED Final Technical Report Sep 79 - May 80
		6. PERFORMING ORG. REPORT NUMBER
7. AUTHOR(s) M. Schulz and K. Blumenstock		8. CONTRACT OR GRANT NUMBER(s) DAJA37-79-C-0547
9. PERFORMING ORGANIZATION NAME AND ADDRESS Institut für Angewandte Physik Universität Erlangen-Nürnberg, Germany		10. PROGRAM ELEMENT, PROJECT, TASK AREA & WORK UNIT NUMBERS 6.11.02A 1T161102BH57-03
11. CONTROLLING OFFICE NAME AND ADDRESS USARDSG-UK Box 65, FPO NY 09510		12. REPORT DATE October 1980
		13. NUMBER OF PAGES 44
14. MONITORING AGENCY NAME & ADDRESS(if different from Controlling Office)		15. SECURITY CLASS. (of this report) Unclassified
		15a. DECLASSIFICATION/DOWNGRADING SCHEDULE

16. DISTRIBUTION STATEMENT (of this Report)

Approved for Public Release; distribution unlimited

17. DISTRIBUTION STATEMENT (of the abstract entered in Block 20, if different from Report)

18. SUPPLEMENTARY NOTES

19. KEY WORDS (Continue on reverse side if necessary and identify by block number)

Semiconductors
MOS Devices
Photo Excitation
MOS Interface States

20. ABSTRACT (Continue on reverse side if necessary and identify by block number)

MOS interface states have been studied in n-type samples by infrared optical excitation. Infrared light in the wavelength range 5 to 15 µm was used to excite only shallow states near the conduction band edge. Thermal background radiation was excluded in the irradiation by using cold interference filters for the spectral selection.

For a sample with low density of states approx. $10^{10} cm^{-2} eV^{-1}$, a consistent

DD FORM 1473 EDITION OF 1 NOV 65 IS OBSOLETE

20.   Contd.

density was observed in the optical measurement with quasistatic measurements and CC-DLTS. The optical absorption cross-section $\sigma_{opt} \approx 3 \times 10^{-19} - 6 \times 10^{-19} cm^2$ assumes low values which are in favor for a model which interprets interface states by tunneling into a discrete level in SiO_2.

Another sample with a high density of states shows a complicated behavior with a field dependence and inconsistency of the density of states observed by different techniques which cannot be completely interpreted. The absorption cross-section, however, also assumes low values below $10^{-18} cm^2$.

10 to the -18th power sq cm.

Accession For

NTIS GRA&I		☑
DTIC TAB		☐
Unannounced		☐
Justification		

By_____

Distribution/

Availability Codes

Dist	Avail and/or Special
A	

OPTICAL EXCITATION OF MOS INTERFACE STATES

Final Technical Report

by

M. Schulz and K. Blumenstock

October 1980

Summary

MOS interface states have been studied in n-type samples by infrared optical excitation. Infrared light in the wavelength range 5 to 15μm was used to excite only shallow states near the conduction band edge. Thermal background radiation was excluded in the irradiation by using cold interference filters for the spectral selection.

For a sample with low density of states approx. $10^{10} cm^{-2} eV^{-1}$, a consistent density was observed in the optical measurement with quasistatic measurements and CC-DLTS. The optical absorption cross-section $\sigma_{opt} \approx 3 \times 10^{-19} - 6 \times 10^{-19} cm^2$ assumes low values which are in favor for a model which interprets interface states by tunneling into a discrete level in SiO_2.

Another sample with a high density of states shows a complicated behavior with a field dependence and inconsistency of the density of states observed by different techniques which cannot be completely interpreted. The absorption cross-section, however, also assumes low values below $10^{-18} cm^2$.

Table of Contents

I Introduction

The measurement techniques most frequently used to analyse
density and properties of MOS interface states are the
quasistatic technique, the conductance technique and recently
CC-DLTS. The properties of interface states are now well
established /1/. A continuum of states is observed with an
increase in density towards the conduction band edge.
The capture cross-section for electrons shows a strong
decay near the conduction band. Results of the conduction
technique and CC-DLTS agree very well /2-4/.

The physical origin of MOS interface states is still
uncertain. Various explanations for the interpretation, e.g.
tunneling into a distribution of traps in SiO_2 and the
charge model, may be ruled out by the measured electrical
properties /3,5/. The properties of interface states may be
explained by a model /5/ which assumes that a discrete
trap level is present in SiO_2, the energy of which is dependent
on the distance from the interface.

The experiment in this report is especially designed to test
this model. In this experiment infrared light is used to
excite interface states especially at low energies in the
vicinity of the conduction band edge where other techniques,
e.g. the conductance technique, are affected by potential
fluctuations. Because the wavelength of the light determines
the energy depth for excitation, this experiment is expected
to be independent of potential fluctuations similar to
CC-DLTS /3/ where the thermal energy determines the energy

position. In the region where the electricalcapture cross-
section drops to low values we also expect a strong decrease
in the absorption cross-section when the model of ref./5/is
valid.

Photoexcitation of MOS interface states has been reported
by Greve et al /6,7/ and Pierret /8/. These measurements
use infrared light of energy $h\nu \geq 0.55eV$, which excites
interface states near midgap or shallow states deep into
the band. In contrast to these experiments, we use light
at wavelength 5 - 15 μm in order to excite shallow states
in the energy region < 0,24 eV where the drop-off of the
capture cross-section is observed. The measurement in this
region requires low temperature measurements and special
measures to remove the room temperature thermal radiation.

II Fundamentals of the Experiment

1. Measurement Principle

The measurement principle is explained in Figs. 1a and b.
In order to fill interface states with charge carriers (electrons
in an n-type substrate) the MOS capacitor is biased into
accumulation (Fig. 1a) by a filling pulse (duration t_p). For
optical excitation of these charge carriers from interface states
by monochromatic infrared light the capacitor is biased into
depletion. Photoexcited carriers are then removed from the inter-
face by the built-in electric field.
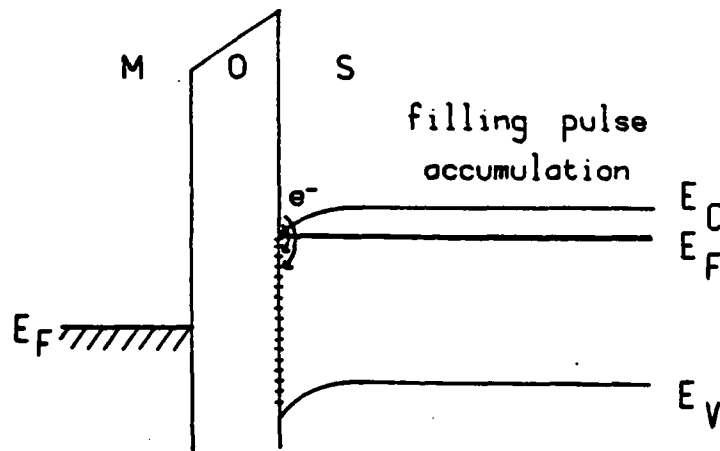
Fig. 1:
Schematic band structure
diagrams

a) Condition during
   filling pulse
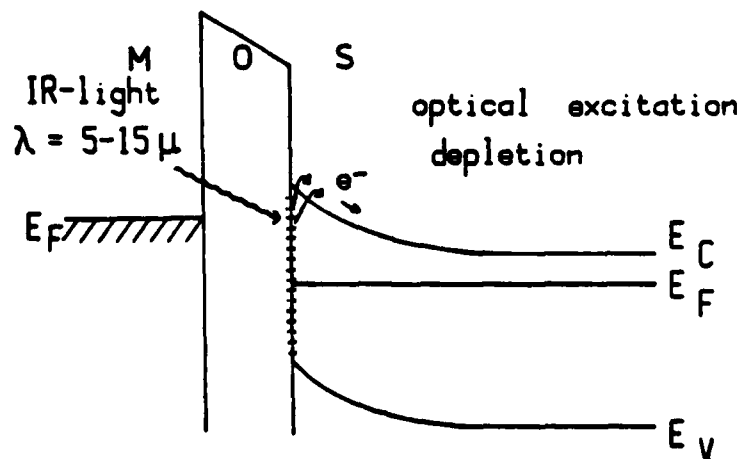
b) Condition for photo-
   excitation. Electrons
   are removed from
   interface by built-in
   field.

The charge change ΔQ in interface states can be monitored by sensitive capacitance measurements.

In the experiment, a technique similar to CC-DLTS is used. The capacitance is kept constant by a feedback of the capacitance signal to the bias voltage. The transient inter- face charge is then monitored by the transient observed in the bias voltage. The capacitance and voltage signals are schematically shown in Figs. 2a and 2b, respectively. During the filling pulse, the feedback is usually switched off. In this region, the capacitance is different from the constant value (indicated by the dots in Fig. 2a). The Fig. 2b shows the voltage pulse and the trailing transient schematically.
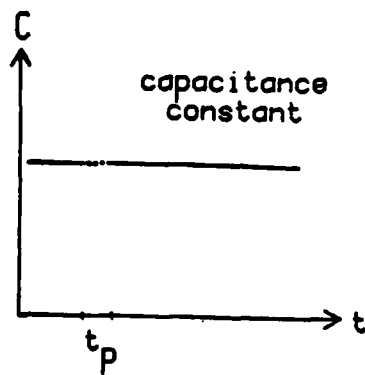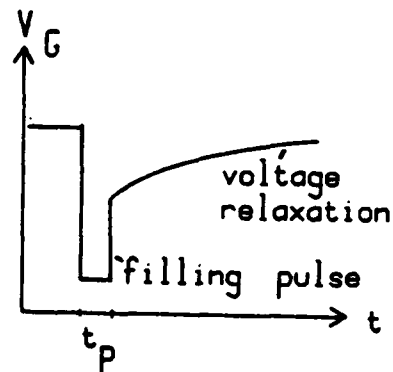
Fig. 2a   Fig. 2b

Fig.2: Schematic drawing of the capacitance variation (a) and voltage variation (b) with time during measurement.

The time needed in accumulation to fill traps is less than 1ms.
In the experiment 1s duration was used for the filling pulse.
The transient of the photoexcitation is dependent on the
photon flux and the absorption cross-section of interface traps.
The transients are very slow, on the order of several hours.
In order to avoid thermal emission during the long transient
for photoemission, the specimen has to be kept at temperatures
as low as possible. The lower limit is given by the RC-constants
which limit the capacitance measurement. The thermal emission
rate is known from transient capacitance measurements /3/.
The emission time constant is given by

$$1/ \tau = \sigma_c \, v_{th} N_c \, \exp \{-(E_c-E)/kT\} \qquad (1)$$

where N_c is the effective density of states in the conduction
band, v_{th} the thermal velocity, σ_c the electron capture cross-
section, k the Boltzmann constant, T the temperature, and
E_c-E the energy depth of the interface state below the conduction
band edge. The dependence of the emission time constant on
energy and temperature is shown in Fig. 3 for a typical capture
cross-section variation as given in the insert. From this
plot it can be visualised that for specimen temperature 45k
and typical observation time for the transient 1000s (dotted
line) all interface states at energies less than E_{th} = approx.0.1eV
have been emptied by thermal emission. The upper energy limit
for photoexcitation is determined by the photon energy
(E_λ = 0.165 eV for λ= 7.5μm in Fig. 3). Interface states
available for photoexcitation are located in the hatched
energy region in Fig. 3. The lower energy boundary E_{th} of the
region may be varied by the sample temperature, the upper limit E_λ

may be varied by the wavelength of the infrared light used
for the optical excitation.
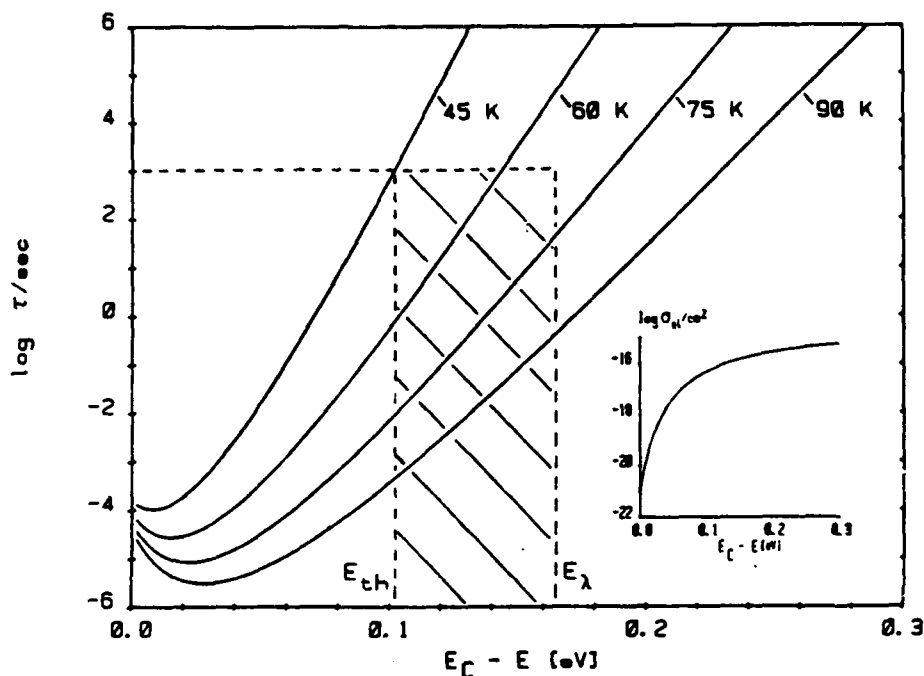
Fig. 3:   Sketch of the time constant variation for thermal emission.
          Parameter is the sample temperature. Only states in the hatched
          energy region are available for the photoemission.

2. Basic Theory for the Evaluation

In order to describe the photoexcitation process, we introduce
an optical absorption cross-section $\sigma_{opt}(E,\lambda)$ which is
a function of the optical wavelength λ and of the energy
position E of the interface state. The pure emission process
is determined by the rate equation

$$dN(E,t)/dt = - N(E,t) \cdot \sigma_{opt}(E,\lambda)\Phi_\lambda \qquad (2)$$

where $N(E,t)$ is the interface state density at energy E occupied by an electron, and Φ_λ is the monochromatic photon flux reaching the interface. The solution of the differential equation is given by

$$N(E,t) = N_{ss}(E) \cdot \exp \{- \sigma_{opt}(E, \lambda) \cdot \Phi_\lambda \cdot t\} \qquad (3)$$

where N_{ss} is the total density of interface states.

The change of charge ΔQ observed in the transient is obtained by integrating over the energy interval $E_{th} - E_\lambda$

$$\Delta Q(t) = \int_{E_{th}}^{E_\lambda} qN_{ss}(E)(1-\exp \{- \sigma_{opt} \cdot \Phi_\lambda \cdot t\}) \, dE \qquad (4)$$

This charge is related to the measured voltage transient $\Delta V(t)$ in the MOS capacitor simply by

$$\Delta V(t) = \Delta Q(t)A/C_{ox} = Aq/C_{ox} \cdot \int_{E_{th}}^{E_\lambda} N_{ss}(E)(1-\exp\{-\sigma_{opt}\Phi_\lambda t\}) \, dE \qquad (5)$$

in the same manner as in CC-DLTS /3/ because the semiconductor space charge region is kept constant.

Equation 5 is used for the evaluation of the experimental data. The parameters $N_{ss}(E)$, Φ_λ, E_{th}, E_λ, and C_{ox} are known by independent measurements e.g. CC-DLTS, and the quasistatic technique. The problem in the evaluation is the unknown

variation of σ_{opt} with energy and wavelength. Approximations
have to be used to extract information on σ_{opt} from the
measured voltage transient $\Delta V(t)$. Details will be discussed
in chapter V, where the experimental data are evaluated.

III Experimental

The experimental apparatus used consists of three main parts:
the low temperature cryostat, the optical system, and the
electronics for the capacitance measurement. These three
parts are decribed separately.

1. Cryostat

A He-flow cryostat is used for the experiment to cool the
sample to a variable temperature in the range 4 - 300 K.
The cross-section of the inner sample chamber with the optical
windows is shown in Fig. 4.

The specimen is mounted in the inner chamber which is filled
with dry He exchange gas. The sample may be illuminated through
two windows in the cold inner and outer wall with a field of
view FOV = 40°. Four windows are installed at right angles
at two sides and in the front and back of the cryostat tube
(see Fig. 5).
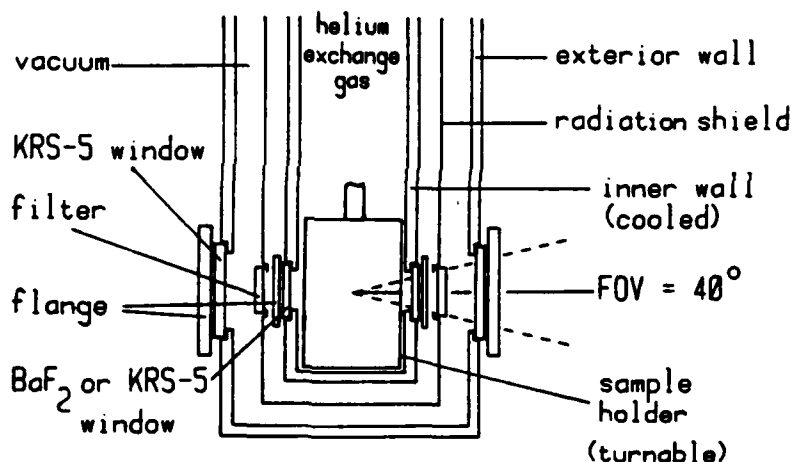
Fig. 4: Cross-section of the sample chamber in the He-cryostat.

The wavelength selection is obtained by interference filters
which are mounted in the cold radiation shield. Four filters
-one for each window- could be installed. A selection of
five interference filters on Ge substrate was available
with data as given in Table 1. The maximum transmission of
the filters varied between 50 and 72%. The pass bands were
chosen to approximately 10% of the center wavelength. Outside

the pass band the transmissivity was checked and found to be
less than 0.5% in the wavelength range 0.3 µm to 17 µm.

λ{µm}	E_λ = hv{eV}	max. transmission in %
4.7 - 5.5	~0.240	52
5.7 - 6.5	~0.206	60
7.3 - 8.2	~0.165	72
9.5 -10.7	~0.124	66
14.5 -16.0	~0.080	53

Table 1: Data of the five different filters.

By the use of cold filters for the wavelength selection,
thermal radiation from the room temperature background is
shielded and only contributes to the radiation in the desired
pass band. A monochromator at room temperature cannot be
used in this experiment because the optical excitation in
the sample integrates the total incident radiation. The room
temperature background radiation would amount to a photon
flux of approx 10^{18} photons $sec^{-1}cm^{-2}$ in the wavelength region
from 5 to 15µm, which is large in comparison to the monochromatic
illumination through the monochromator.

For the infrared transparent windows BaF_2 and KRS 5 has been
used. The vacuum seals for the inner cold windows caused
problems because of the soft material and the different
thermal expansion in the wide temperature range used for the
experiments. One KRS 5 window was therefore only installed in

connection with the filter at the longest wavelength. The
transmission of this window is 72% in the range 0.65 to 30μm.
With the other three filters, BaF_2 windows having a transmission
of 92% (0.3-9μm) could be used .

An Indium vacuum seal was satisfactory for the BaF_2 windows.
Silicone resin (Vacseal) was used for the KRS 5 window.
Four KRS 5 windows were installed in the outer wall.

2. Optical System

In order to reduce the transient time of the emission,
a monochromatic photon flux as large as possible is
needed in the wavelength region 5 to 15 μm. In our experiment,
we used a globar as a source with a large - aperture optical
mirror system as shown in Fig. 5. The optical system was
mounted on a table which could be rotated so that the four
different windows of the cryostat could be illuminated.
Different optical wavelengths are therefore available for
the infrared excitation.
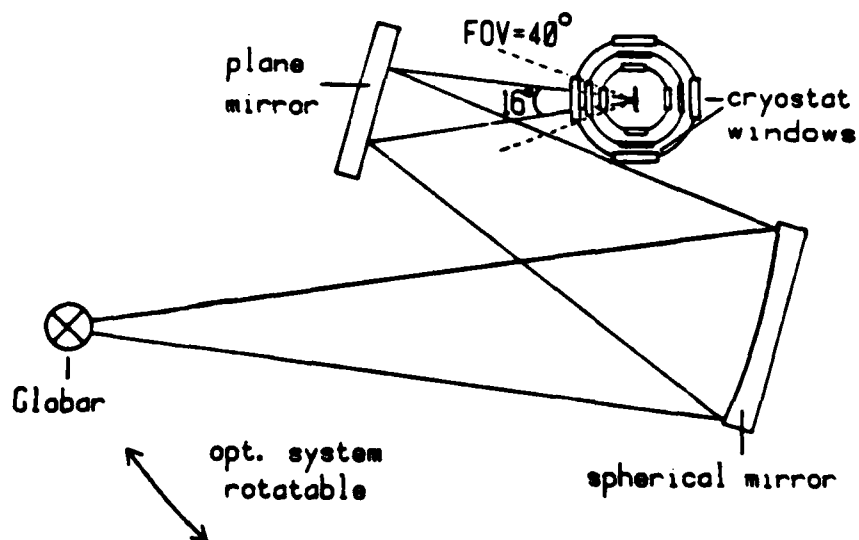
Fig. 5: Outline of the infrared optical system for illumination.

Two Al-coated mirrors are used to focus the radiation of the globar on the sample. The aperture of the optical system is only 16° so that thermal background radiation with FOV 40° and light from the globar both contribute to the irradiation on the sample.

The globar was operated at 34 Volts and 14 Amps. The relative emission spectrum of the globar was measured by an infrared spectrometer. The result is shown in Fig. 6. The total photon flux reaching the interface of the sample may be calibrated by using the sample itself as a detector and the room temperature background 300 K radiation with the FOV = 40° as a calibrated

light source. This background radiation is assumed to be from a
black body source (emissivity $\epsilon = 1$) at 300 K. For this radiation
source, the photon flux reaching the sample can be calculated
with the known transmissivity of the windows and the data of
the filters. The values for the background photon flux reaching
the sample are listed in Table 2 for the five filters used.
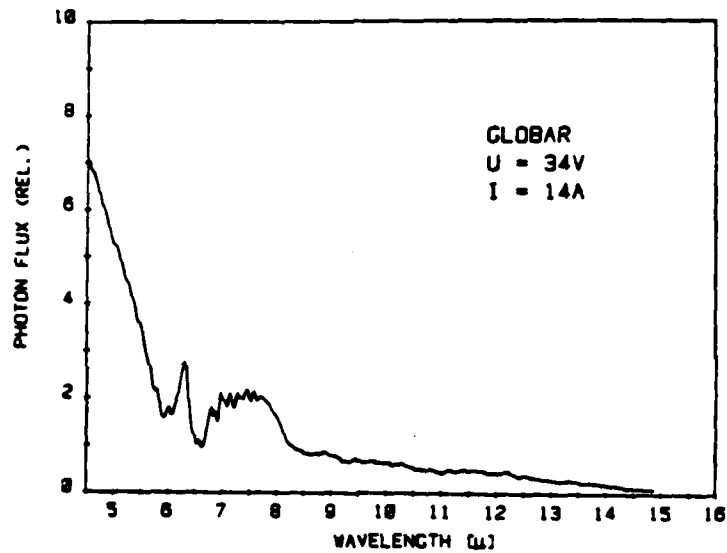
Fig. 6: Relative emission spectrum of globar IR-light source in
wavelength region 5-15μm.

The photon flux generated by the globar ϕ_G was determined by
the relation to the background flux ϕ_B

$$\phi_G(FOV = 16°) = (\frac{\Delta V_G - \Delta V_{th}}{\Delta V_B - \Delta V_{th}} - 1) \; \phi_B \; (FOV = 40°)$$

The photo-signal ΔV in the capacitor was measured for the
illumination with the globar ΔV_G and with just the thermal
background radiation ΔV_B . Both signals have to be corrected

by the signal obtained for pure thermal emission V_{th}.
This measurement was taken for the 7.5μm filter. The
increase of the photon flux is approximately 50%. Values
of the photon flux obtained by the globar are also listed
in Table 2. The values for the other four filters are
obtained from the relative emission spectrum in Fig. 6.
For the long wavelength filters, the increase of the photon
flux by using the globar is marginal. At the short wavelengths
5 μm and 6 μm, the use of the globar is effective.

Filter (μm)	ϕ_G(FOV = 16°) (cm^{-2}sec^{-1})	ϕ_B(FOV = 40°) (cm^{-2}sec^{-1})
5	$8.9 \cdot 10^{14}$	$1.4 \cdot 10^{14}$
6	$4.3 \cdot 10^{14}$	$4.0 \cdot 10^{14}$
7.5	$5.5 \cdot 10^{14}$	$1.1 \cdot 10^{15}$
10	$1.9 \cdot 10^{14}$	$1.9 \cdot 10^{15}$
15	$3.6 \cdot 10^{13}$	$2.2 \cdot 10^{15}$

Table 2: Photon flux of the globar and background photon flux
for the five filters. The error of ϕ_G is approximately
± 70%, the error of the background photon flux is less
than 20%.

In an earlier experiment a Cr-Ni filament was used as a light
source. Because of the lower temperature (1400 K instead of
1800 K for the globar) this infrared light source was even
less effective.

The photon flux reaching the interface Si-SiO$_2$ is dependent on
the structure of the sample. The further reduction will be
discussed in chapter III 4.

3. Electronics

The block diagram of the electronic regulation and measurement
is shown in Fig. 7. The capacitance of the sample is measured
by a standard 1 MHz capacitance meter. The high-frequency
measurement of the capacitance limits the lowest possible
sample temperature because the series resistance of the sample
increased at low temperatures due to the freeze-out of the
electrons. The lowest temperature 45K was determined
experimentally.
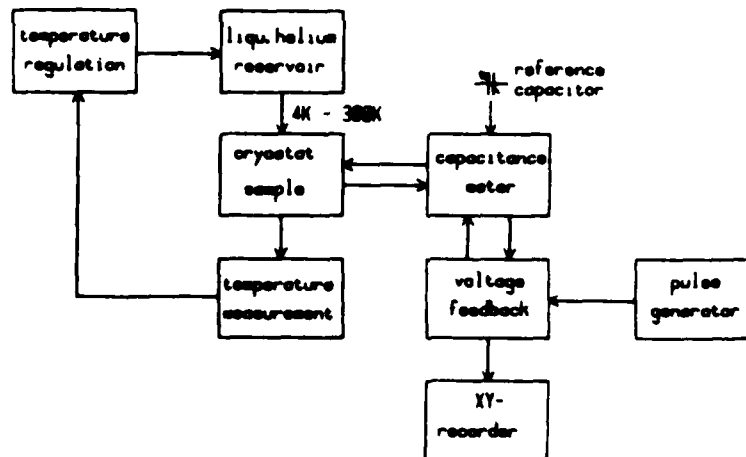
Fig. 7:
Block diagram of
electric regulation and
measurement system.

The bias voltage was applied to the sample through a filter
circuit in the bridge. The steady state capacitance of the
sample was balanced by a variable reference capacitor so that
a high gain could be used in the feedback loop of the
capacitance signal to the voltage supply.

During the filling pulse (approx. 1ms to 1s) the feedback is
switched off so that accumulation can be reached. The voltage

transient after the pulse with a constant capacitance maintained
by the feedback regulation is directly recorded by an x-y-
plotter. For low densities of interface states,the signal
in the voltage transient may be very small,less then 1mV.
It is therefore necessary that very stable power supplies
with a drift less than 1mV/hour are used. CC-DLTS measurements
and quasistatic CV-measurements are taken separately with
an apparatus described elsewhere /2,3/..

The temperature of the He-flow crystat is constant to within 0.5K by
controlling the He-flow and the heater power electronically.
The chamber temperature and sample temperature were separately
measured.

4. Sample Preparation
Only results obtained on MOS capacitors on n-type Si substrates
are reported. A typical structure is shown in Fig. 8. The
substrate material was 4-6 Ohm cm phosphorous-doped,100-
oriented bulk silicon. Thermal oxidation was performed at
1000°C to an oxide thickness of approx 1000 Å.
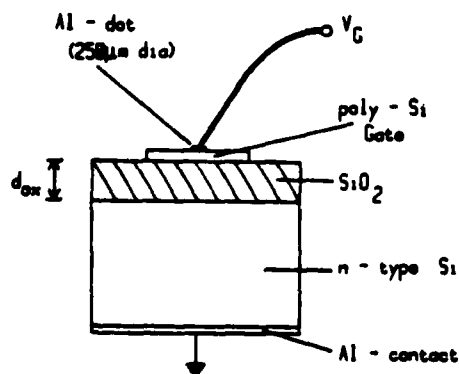
Fig. 8:
MOS sample structure

There are three possibilities for the infrared light to
reach the interface region:

-an infrared transparent gate electrode (e.g. poly-Si) is
 used. The sample is illuminated on the front face through
 the gate

-the sample is illuminated on the back contact. The in-
 frared light reaches the interface under the gate electrode
 through a window in the back contact and through the bulk
 substrate

-the sample is illuminated on the front face between the
 isolated gate electrodes. The infrared light reaches the
 interface under the gate electrode by multiple reflection
 and scattering of the light in the sample.

It will be shown in chapter VI that the photon flux reaching
the interface for the last procedure is too low so that
no measurements could be taken.

Measurements were taken by the first procedure with a
transparent gate electrode. A poly-Si layer 0.5µm thick and
nominally undoped was used. The samples were prepared for us
by G. Sixt at AEG-Telefunken, Heilbronn. The assistance is
gratefully acknowledged. Gate electrodes 1mm² were prepared
from this layer. In order to obtain a good electrical
contact to the poly-Si layer, a small Al dot was evaporated.

The infrared transmissivity of these layers is reported
in the literature /9/. We used the reported data for the
transmissivity of the poly- Si gate plus the SiO_2 to determine
the fraction of the photon flux at the sample which reaches the
interface. The values of transmission used for the wavelengths
of the filters and of the photon flux which reaches the
interface is listed in Table 3.

Filter {μm}	Transmissivity	$\Phi_\lambda \{cm^{-2} sec^{-1}\}$
5	0.53 ± 0.05	$(1.1 \pm 0.7) \cdot 10^{15}$
6	0.60 ± 0.05	$(1.0 \pm 0.5) \cdot 10^{15}$
7.5	0.67 ± 0.04	$(2.3 \pm 0.8) \cdot 10^{15}$
10	0.78 ± 0.01	$(3.1 \pm 0.8) \cdot 10^{15}$
15	0.76 ± 0.01	$(3.5 \pm 0.8) \cdot 10^{15}$

Table 3: Photon flux Φ_λ at the interface. The values are
calculated with both the errors of the globar
and background photon flux. Reflexion at the back
contact was taken into account.

Results will be shown for two different samples, A and B.
Sample A received the usual anneal at 450°C in hydrogen
ambient for 30 minutes. Sample B received an additional
anneal at 550°C after deposition of the poly-Si and before
Al-evaporation of the back contact in order to reduce the
interface state density.

The sample holder in the cryostat is shown in Fig. 9. The
sample is mounted on a gold plated BeO plate for good
thermal contact and electrical insulation. A phosphorous bronze
spring with a brass plunger and plastic tip presses the wafer
down on to this plate. The back "low" contact of the sample

is soldered to the gold plating of BeO plate. The "high"
contact is obtained by a Pt tip to the Al dot on the poly-Si
gate electrode. The shaded area of the Al dot and the wire
is negligible.
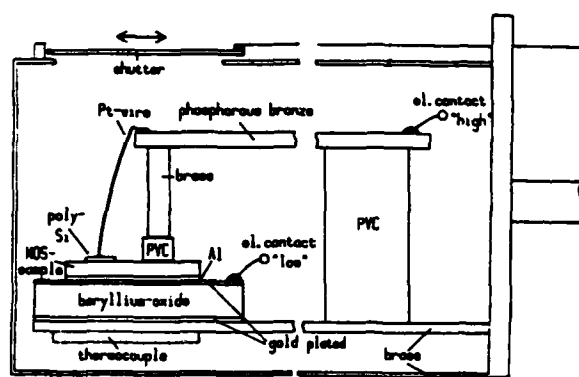
Fig. 9:
Sample holder in the
He-cryostat.

The sample is completely screened from thermal radiation and
electrical·stray fields by a brass can. An electromagnet
opens a cold shutter for irradiation. The sample holder can
be rotated in the cryostat so that the sample faces the
optical window with the filter for the desired wavelength.

IV Measurement Results

In this chapter measured results are presented. For the
samples A and B under investigation detailed CV-measurements
have been performed in order to determine the relation of the
surface potential Ψ_s to capacitance and bias voltage /1/.
Interface state densities have also been determined by CC-
DLTS /5/. CV-measurements have been taken at room temperature
and at low temperatures where photoexcitation is.observed.

1. CV-Measurements

The Figs. 10a and b show CV-measurements for the samples A
and B at room temperature and at 45K and 50K, respectively.
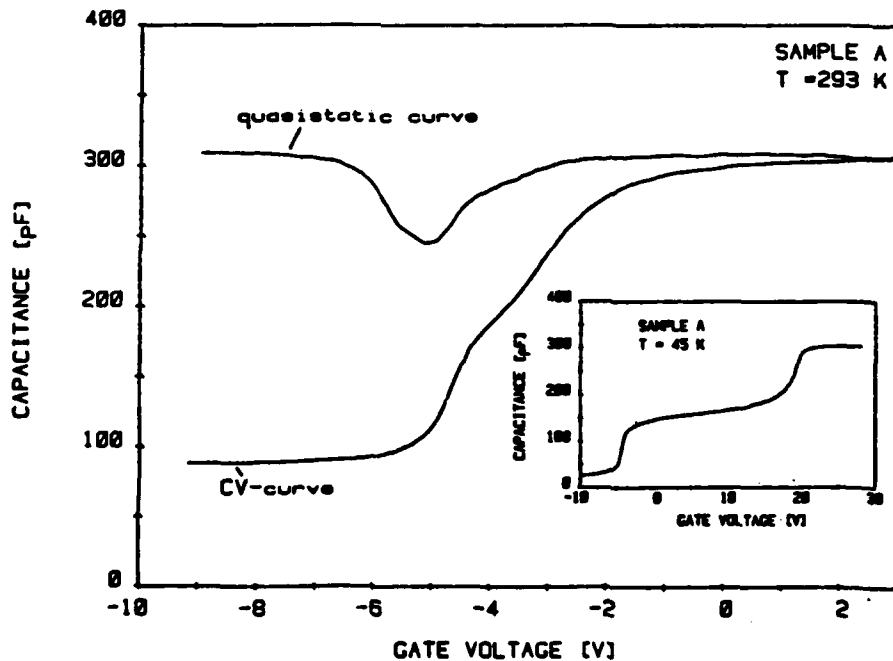
Fig. 10a: Result of CV-measurement of sample A at room temperature
and at 45 K in the insert.
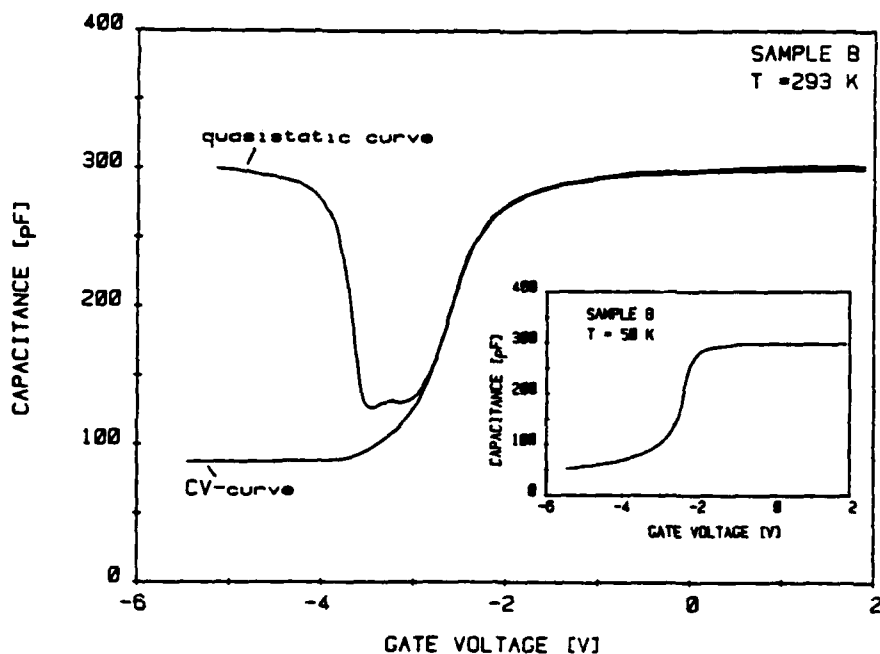
Fig. 10b: Result of CV-measurement of sample B at room temperature and at 50K in the insert.

Sample A shows a large separation of the low (quasistatic) and high-frequency measurement, indicating a larger interface state density than sample B where the separation is smaller. The flat band voltage U_{FB} = -2 Volt is approximately the same in both samples.

The result obtained at low temperature is completely different. Sample B shows normal behavior. The lack of an inversion layer at low temperatures leads to deep depletion at negative bias voltages in excess of -3 Volts.

Sample A shows a huge flatband voltage shift of 20 Volts at low temperature indicating a large density of acceptor states in the vicinity of the band edge. Large bias pulses >30Volts are necessary to reach accumulation at low temperatures for this sample.

The result of CC-DLTS measurements on samples A and B
are shown in Figs. 11a and b. In this measurement, filling
pulses of 1ms duration and sampling delay times of 10 and
20 ms were used. The density of states determined by the
two techniques agree within the error of the measurement.
Sample A shows a steep increase towards the conduction band.
The magnitude of the density of states is high.

Sample B shows a low density of states around or less than
10^{10} cm^{-2}eV^{-1}. For this low density, the quasistatic technique
is not very accurate. The observed dip at -0.3 eV is not real.
It can be explained by potential fluctuations /1/.
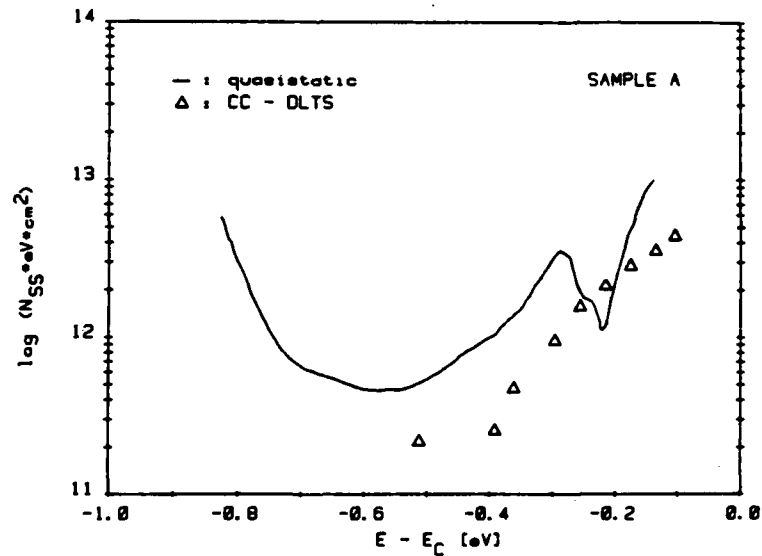
Fig. 11a: Interface state density as a function of energy for sample
A as determined by quasistatic CV-technique (continuous line)
and CC-DLTS (triangles)
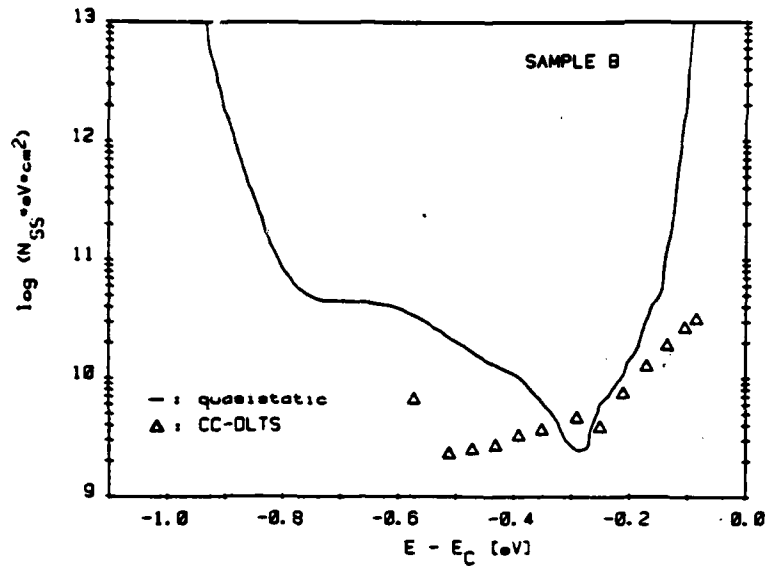
Fig. 11b: Interface state density as a function of energy for sample B
as determined by quasistatic CV-technique (continuous line)
and CC-DLTS (triangles)

2. Optical Excitation

Typical transients of the infrared optical excitation are shown
in Fig. 12 a, b, c.
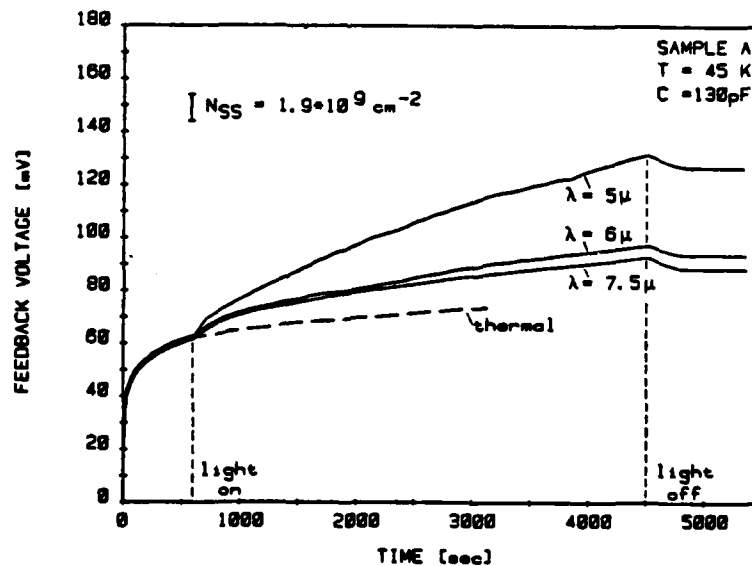
Fig. 12a: Measured transients for photoexcitation in sample A with
constant capacitance C = 130pF.
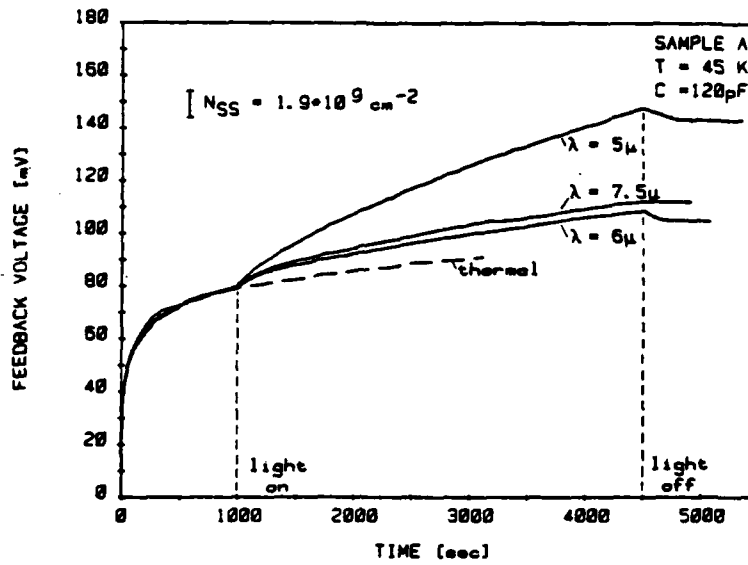
Fig. 12b: Measured transients for photoexcitation in sample A with constant capacitance C = 120 pF.
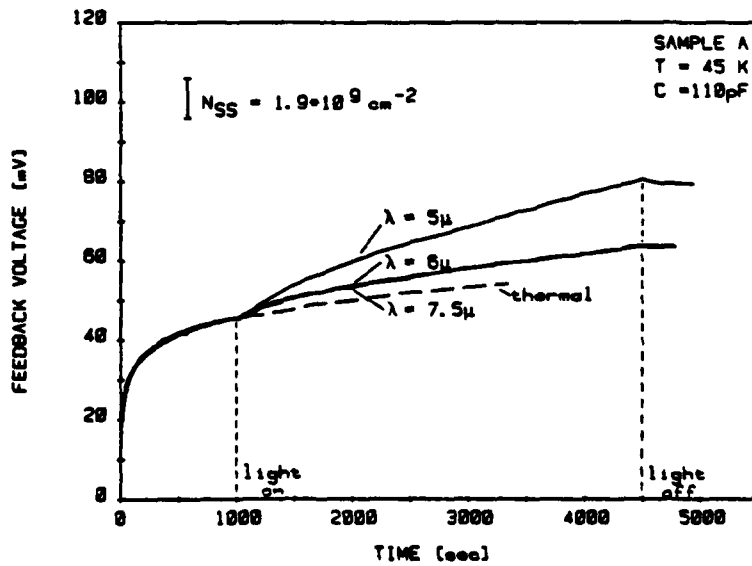
Fig. 12c: Measured transients for photoexcitation in sample A with constant capacitance C = 110 pF.

The feedback voltage is shown as a function of time after the
filling pulse. The calibration of the scale to density of
states is given in the insert. The transient due to pure
thermal emission is shown by the dashed line. The shutter
is usually opened after about 600s to turn on the irradiation
when the initial thermal emission of shallow states has passed.
The increase of the emission due to photoemission is clearly
visible. A strong dependence on the wavelength is observed.
When the irradiation is stopped by closing the cold shutter, a
constant level is reached after a short transient.

The parameter changed between Figs.12a and c is the constant
capacitance. Values between 130 pF and 110pF have been chosen.
The magnitude of the optical effect is clearly smaller for
smaller capacitances. The ratio of the signals for different wavelengths is
unchanged. This behavior is not expected from the basic
principle of the experiment, as explained in chapter II.

The strong effect of the temperature is shown in Fig. 13.
With increasing temperature the lower limit of the energy
region E_{th} is increased, thus reducing the number of states
for the photoexcitation. The expected reduction of photo-
excitation with increasing temperature is clearly visible in
Fig. 13.
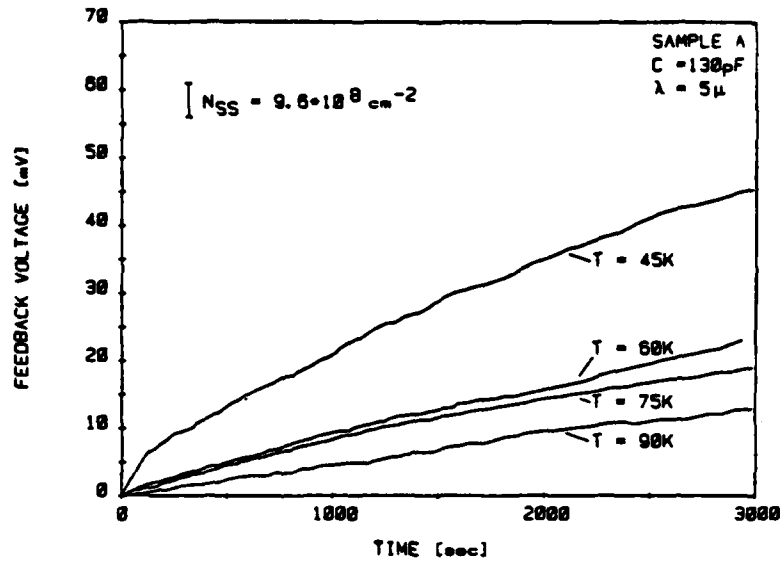
Fig. 13.: Measured transients for photoexcitation in sample A with temperature as varied parameter. Other data as shown in insert.

The result observed for sample B is shown in Fig. 14. The observed signal is much smaller than for sample A because of the low density of interface states. The effect of the light, however, is clearly visible. The wavelength dependence is weak.
The variation with the capacitance (Fig. 15) is negligible.
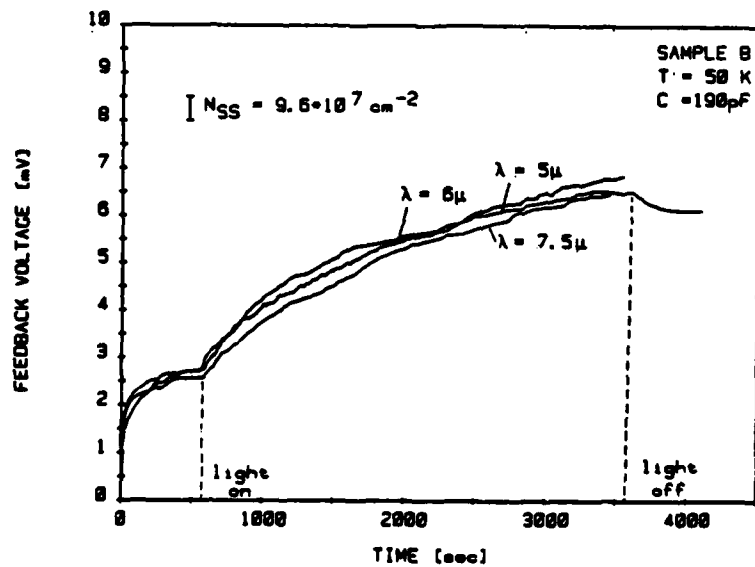
Fig. 14: Measured transients for photoexcitation in sample B. Parameter is the wavelength for excitation. Other data as shown in insert.

-29-
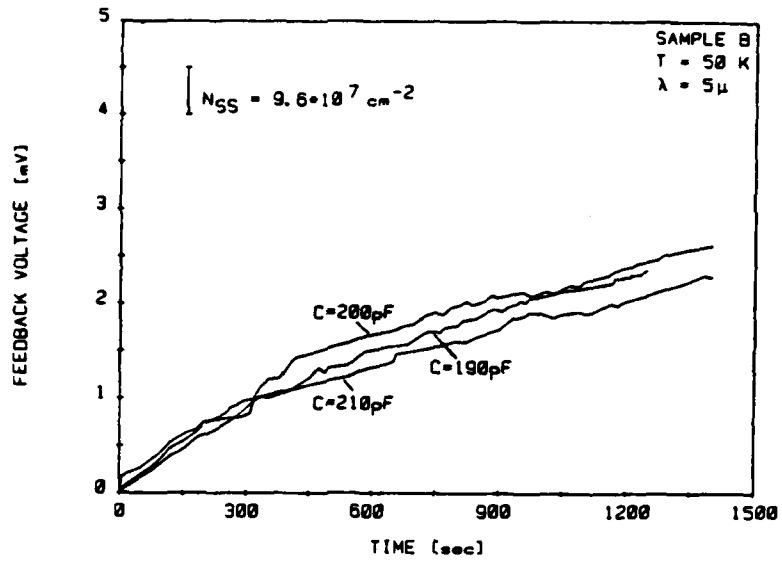
Fig. 15: Measured transients for photoexcitation in sample B. Parameter varied is the constant capacitance. Other data as shown in the insert.

The measurement could only be taken at 50 K. At temperature 60 K, no photoexcitation signal could be resolved, even for excitation with light at 5µm.

V Discussion

The results of the measurements presented in chapter IV show
the expected qualitative behavior. Superimposed on the thermal
emission of charge trapped in interface states, the additional
photoemission is clearly observed. A saturation of the emission
which would make the evaluation easy could not be observed
although long observation times of up to several hours have
been used. A direct quantitative determination of the density
of states in the energy range $E_\lambda - E_{th}$, as discussed in chapter II,
is not possible. A quantitative evaluation therefore has to be
based on the time dependent integral of eq. 5.

The evaluation of this equation is complicated because the
optical cross-section in the exponent of the integrand and
its dependencies with energy and wavelength are not known and
can only be obtained by a computer fit of the equation 5. The
accuracy of the measurement of the two samples investigated is
not high enough, that the full variation can be fitted. In
sample A, having a high density of states, the flatband
voltage shift observed (>20 Volts) is so large, that a large
fluctuation of the surface potential can also be expected,
which strongly affects the measurement. The relation of eq. 5
is only valid for the case $(E_\lambda - E_F)/q > \Delta \Psi_s$ where potential
fluctuations do not affect the measurement.

For sample B, having a low interface state density and a
negligible flatband voltage shift, the potential fluctuations
may be assumed to be as small as required. In this sample,
however, the measurement signal unfortunately is very small,
so that the limits of the sensitivity are reached. In this

case the error in the measurement is so large that a quantitative
detailed fit of an energy and wavelength dependent absorption
cross-section is not sensible. An ideal sample for this
measurement should show an interface state density of a few
times $10^{10} cm^{-2} eV^{-1}$ in midgap.

We used a crude approximation for the quantitative evaluation
of the results for the two samples which have been measured.
We assumed a constant optical absorption cross-section. With this
assumption eq. 5 simplifies to

$$\Delta V(t) = (Aq \cdot N^*_{ss}/C_{ox}) \ (1-\exp \ \{- \ \sigma_{opt} \cdot \dot{z}_\lambda t\} \ ) \qquad (7)$$

where N^*_{ss} $\{cm^{-2}\}$ is a total interface state density which takes
part in the photoexcitation. This total interface state density
and the absorption cross-section can be easily obtained by
a fit of eq. 7 to the measured   transient.

The computer fit is shown in Figs. 16a to c for sample A.
In this measurement the constant capacitance was the
varied parameter. Figure 17 shows the fit to sample A for
all the transients where the temperature was the parameter
varied. The wavelength variation of sample B is shown in
Figs. 18 a to c. Separate plots had to be used for a clear
presentation because the transients only show a small variation.

For all the curves, the exponential fit of eq. 7 is a
satisfactory approximation to the measured transient. The
values obtained for the density N^*_{ss} and the optical cross-
section σ_{opt} from the computer fit are listed in Table 4.
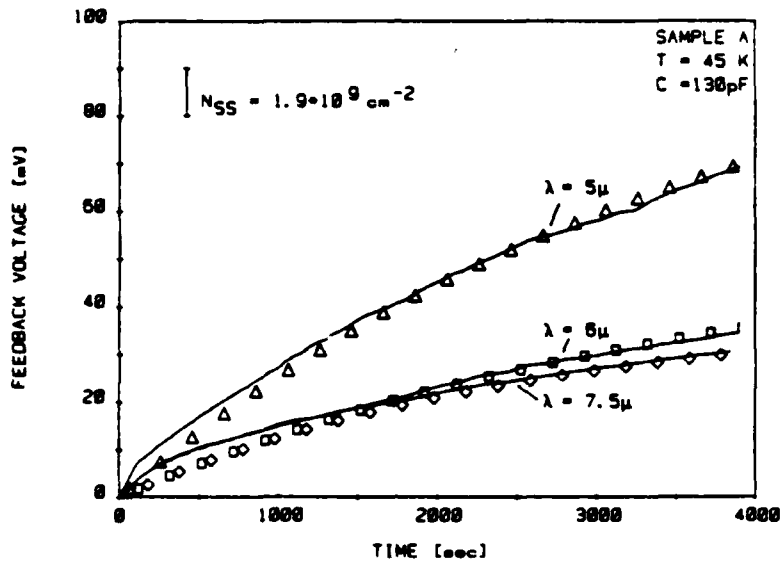
Fig.16a: Computer fit for sample A at C=130pF. The continuous lines are
the measurements, the triangles, squares and rhombs the calculated
fits.
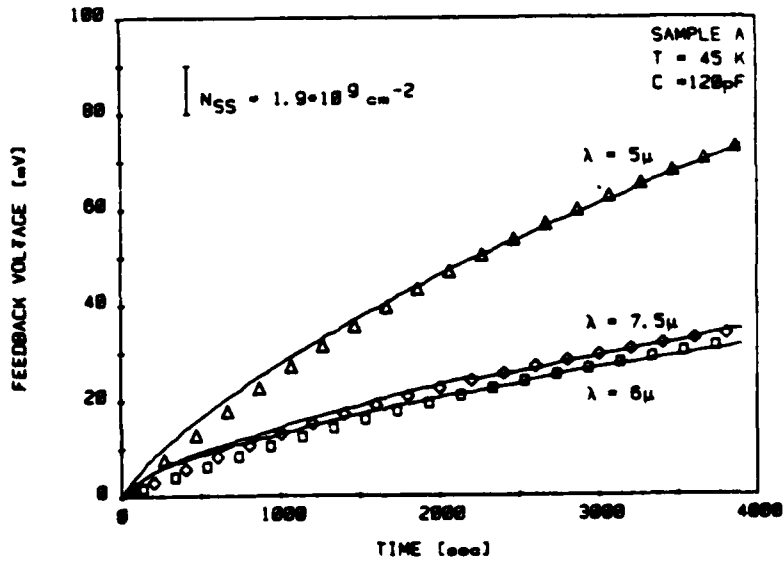
Fig. 16b: Computer fit for sample A at C=120 pF. The continuous lines are
the measurements, the triangles, squares and rhombs the calculated
fits.
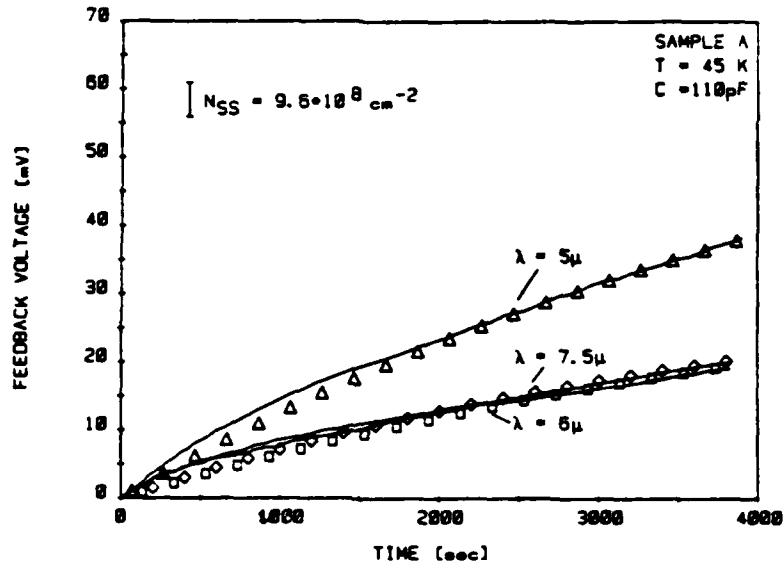
Fig. 16c: Computer fit for sample A at C = 110 pF. The continuous
lines are the measurements, the triangles, squares and rhombs
the calculated fits.
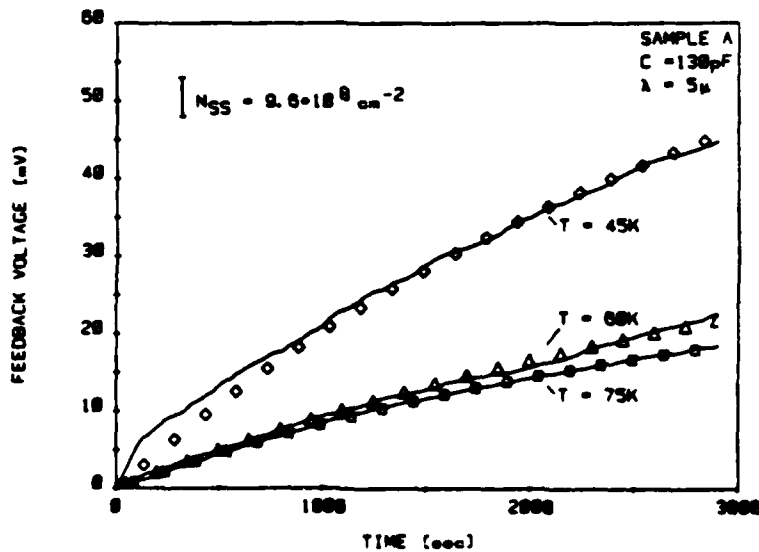
Fig. 17: Computer fit for sample A at different temperatures.
The continuous lines are the measurements, the triangles, squares
and rhombs the calculated fits.

$N_{SS} = 9.6 \cdot 10^7 \, cm^{-2}$

SAMPLE B
T = 50 K
C = 190pF

FEEDBACK VOLTAGE (mV)

$\lambda = 5 \mu$

TIME (sec)
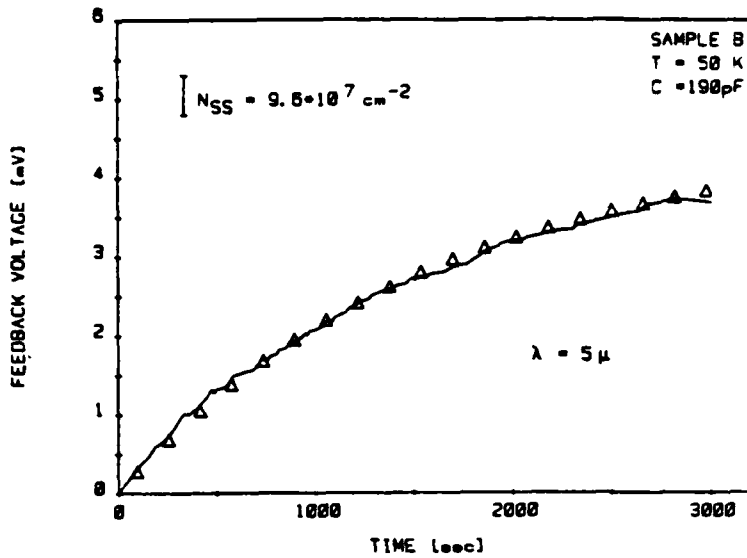
Fig. 18: Computer fit for
sample B at C=190pF.
The continuous lines are the
measurements, the triangles,
squares and rhombs the
calculated fits.

Fig.18a:
Fit for the wavelength λ=5μm

$N_{SS} = 9.6 \cdot 10^7 \, cm^{-2}$

SAMPLE B
T = 50 K
C = 190pF

FEEDBACK VOLTAGE (mV)

$\lambda = 6 \mu$

TIME (sec)
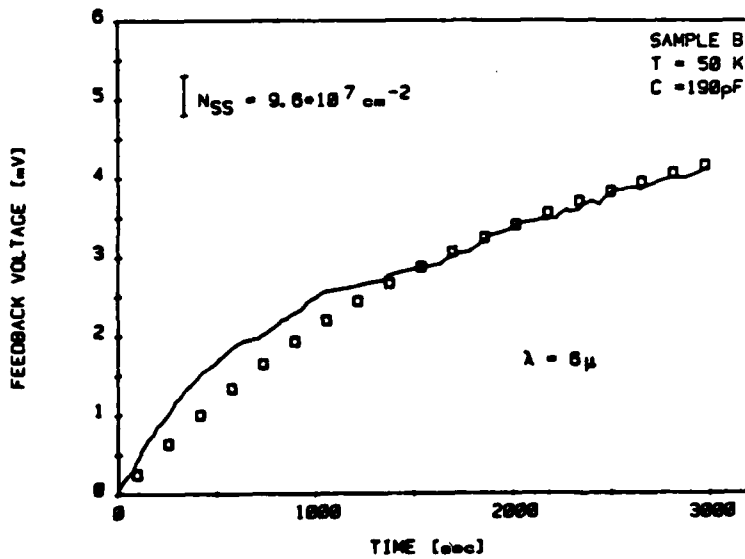
Fig.18b:
Fit for the wavelength λ=6μm

$N_{SS} = 9.6 \cdot 10^7 \, cm^{-2}$

SAMPLE B
T = 50 K
C = 190pF

FEEDBACK VOLTAGE (mV)

$\lambda = 7.5 \mu$

TIME (sec)
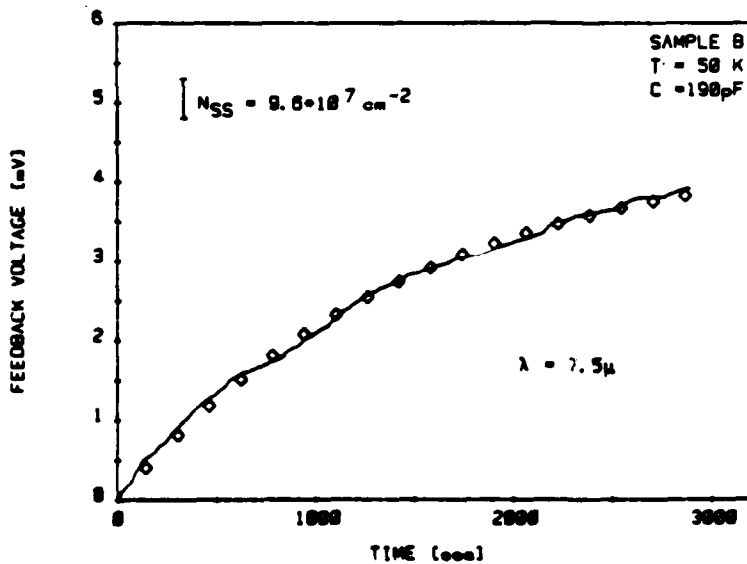
Fig. 18c:
Fit for the wavelength λ=7,5μ

We now give a detailed discussion of the measurements
presented in chapter IV.
Sample B, with the low interface state density, will be
discussed first.

For the good sample B, the N_{ss}^* values determined do not vary
with the variation of the wavelength of the light. A constant
value $N_{ss}^* \approx 1 \times 10^9 cm^{-2}$ is observed. This leads to the conclusion
that in this sample states in the same energy interval are
excited independent of wavelength and that this interval
must be less or equal to the smallest energy region $E_\lambda -E_{th}=$
0.165 eV - 0.112 eV. This conclusion is consistent with the
observation that the signal vanishes for the higher temperature
60K which leads to E_{th} = 0.161eV $\approx E_\lambda$.

The density of states N_{ss}^* can be compared with the inter-
face state density observed by CC-DLTS integrated in the
energy interval E_{th} to E_λ. This value is listed in the last
column of table 4. Good agreement is observed for the wave-
length 7.5 µm. A disagreement is obtained for the larger
energy intervals for wavelengths 6µm and 5µm. It seems that
states deeper in the bandgap are less probable for photo-
excitation because the absorption cross-section assumes small
values. This conclusion is consistent with the measured
wavelength variation of the absorption cross-section,which
shows the largest values σ_{opt}= 6 $\times 10^{-19} cm^2$ at the short
wavelength, 5µm.

A decrease of absorption cross-section was reported by Greve /6/
for deep states at E = 0.21 eV and 0.36 eV and photon energies
varying in the range 0.55eV to 0.88eV.

Our observations show the same trend of a decrease of the absorption cross-section in the long wavelength region. For a fixed wavelength, deep states near E_λ show a lower cross-section for excitation.

This observed energy dependence of σ_{opt} seems to be contradictory to the assumption of a constant absorption cross-section in the evaluation. The evaluation of the measured data, with the crude assumption of a constant absorption cross-section, is possible because of the limited observation time and because the absorption cross-section enters the equ.7 in the exponential. The value obtained for the cross-section is an average in the energy region which determines N_{ss}^* (e.g. E_{th} = 0.112 eV to E=0.165 eV).

In the good sample B, we do not observe a field dependence of the photoemission in contrast to reported results /10/. This field independence was difficult to observe. Possible errors in the measurement which may lead to an interpretation by a field dependence are discussed in chapter VI.

Sample A:
Because the transient in sample A is dependent on the constant capacitance at which the measurement was taken, three values for N_{ss} and σ_{opt} are listed in table 4 for each wavelength. Variations are visible in the density of states as well as in the absorption cross-section when the capacitance is varied. The capacitance variation from 130 pF to 110pF corresponds to a variation of the energy position of the fermi level from 0.52 eV to 0.62 eV from the conduction band edge. The origin

of the variation of the transient signal with bias condition is not understood. It is noted, however, that the same decrease of the absorption cross-section with increasing wavelength is observed.

In the same manner as for sample B, the total density of states N_{ss}^* in the energy interval $E_{th}-E_\lambda$ is calculated from the density of state measurement shown in Fig. 11a and listed in the last column of table 4. This density is more than an order of magnitude higher than the value observed in the optical excitation. In order to check this effect, we have performed a CC-DLTS evaluation of the slow thermal transient (time constants 400 sec, 800sec, 1600sec) shown in Fig. 12c for 45K and higher temperatures 60K, 75K and 90K. This CC-DLTS-evaluation determines interface state densities at temperatures 35K lower than the fast DLTS (10msec, 20msec). The values determined for the density of states N_{ss}^* in the same energy interval $E_{th}-E_\lambda$ are shown in table 4 in brackets. These values are of the same order of magnitude as observed in the optical measurement. It therefore seems that at low temperature interface states disappear from the measurement. We do not have an explanation for this observation.

In contrast to sample B, the temperature variation of the transients could be analysed in sample A. The values determined for the absorption cross-section and total density of states in the optical excitation are included in Table 4.

The absorption cross-section does not vary with temperature
within the error of the measurement.

The total density of states N_{ss}^* decreases with increasing
temperature, as expected, because the energy interval is
reduced. Values for 90K are not listed in table 4, although a
measured transient is still shown in Fig. 13. At 90K
E_{th} = 0.248 eV is larger than E_λ = 0.240 at 5 μm. That
the transient signal has not completely vanished can be
explained by potential fluctuations. Since the fermi level
at 130 pF is located near midgap (0.55eV), and we are
observing interface states at 0.24 eV, we may conclude that
potential fluctions must exceed 0,3 Volts in this sample.
The potential fluctuations cannot be much larger because the
temperature effect, e.g. shift of E_{th} is clearly observed.

It is noticed that the ratio of the density of states in the
fast and slow CC-DLTS evaluation is reduced at higher temperatures.
(11 at 45K to 7.7 at 75K) indicating again the disappearance
of interface states in the measurement at low temperatures.

	Filter (μm)	$E_T...E_\lambda$ (eV)	Capacitance (pF)	σ_{opt} (cm²)	N_{ss}^* (cm⁻²)	$N_{ss}^* = \int_{E_{th}}^{E_\lambda} N_{ss}(E)dE$ (cm⁻²) CC-DLTS
				OPTICAL MEASUREMENT		
SAMPLE A T=45K	5	0.103...0.240	130 / 120 / 110	$2,4\cdot10^{-19}$ / $2,1\cdot10^{-19}$ / $1,7\cdot10^{-19}$	$2,1\cdot10^{10}$ / $2,4\cdot10^{10}$ / $1,5\cdot10^{10}$	$4,2\cdot10^{11}$ $(3,8\cdot10^{10})$ *
	6	0.103...0.206	130 / 120 / 110	$2,6\cdot10^{-19}$ / $2,2\cdot10^{-19}$ / $1,8\cdot10^{-19}$	$1,1\cdot10^{10}$ / $1,1\cdot10^{10}$ / $7,5\cdot10^{9}$	$3,5\cdot10^{11}$ $(2,9\cdot10^{10})$*
	7,5	0.103...0,165	130 / 120 / 110	$1,8\cdot10^{-19}$ / $1,4\cdot10^{-19}$ / $1,1\cdot10^{-19}$	$7,5\cdot10^{9}$ / $9,4\cdot10^{9}$ / $6,4\cdot10^{9}$	$2,4\cdot10^{11}$ $(1,5\cdot10^{10})$*
SAMPLE A 45K/60K/75K	5	0,103...0.240 / 0,161...0,240 / 0,204...0.240	130 / 130 / 130	$2,8\cdot10^{-19}$ / $2,3\cdot10^{-19}$ / $2,9\cdot10^{-19}$	$1,6\cdot10^{10}$ / $8,0\cdot10^{9}$ / $6,0\cdot10^{9}$	$4,2\cdot10^{11}$ $(3,8\cdot10^{10})$* / $1,9\cdot10^{11}$ $(2,2\cdot10^{10})$* / $7,7\cdot10^{10}$ $(1,0\cdot10^{10})$*
SAMPLE B T = 50K	5 / 6 / 7,5	0,112...0.240 / 0,112...:0.206 / 0,112...:0,165	190 / 190 / 190	$5,9\cdot10^{-19}$ / $4,9\cdot10^{-19}$ / $3,0\cdot10^{-19}$	$9,8\cdot10^{8}$ / $1,06\cdot10^{9}$ / $9,1\cdot10^{8}$	$1,6\cdot10^{9}$ / $1,4\cdot10^{9}$ / $9,8\cdot10^{8}$

TABLE 4: Values for interface density N* and absorption cross-section σ_{opt} obtained by the computer fits for the two samples. The interface density can be compared with the values obtained by CC-DLTS integrated in the energy interval E_{th} to E_λ.

*see text

VI Measurement Problems

Before reliable experimental results could be obtained
serious problems occurred in the measurement which are
briefly explained in this chapter:

Stray Light

It is very important that light at wavelengths shorter than
the passband of the filter is excluded from the cryostat
chamber. Even a small fraction of stray light at short wave-
length causes a transient because the absorption cross-section
increases at short wavelengths.

The effect of stray light at short wavelength is visible in
a strong field dependence of the transient and a large
relaxation when the irradiation is terminated. In the
initial experiments stray light reached the sample. A
typical result of the measurement is shown in Fig. 19.
A large transient is observed. The amplitude of the transient
increases with a decreasing capacitance in contrast to
sample A where just the opposite variation is observed.
The high signal amplitude, the field dependence, and the
relaxation occur because light at short wavelengths excites levels
throughout the bandgap above and below the fermi level. The
effects could be removed by closing the leak of the light.

Fig. 19: Effect of stray light for different capacitances. A large
amplitude and a strong relaxation when the light was turned off
is clearly visible.

After this observation, we carefully checked all the filters
for leakage. The three filters used (5µm, 6µm, and 7,5µm)
did not show large relaxations when the light was turned off.
The filter at 10µm showed a relaxation. It was therefore
rejected from the measurements. The filter with center wavelength
at 15µm could not be used because with the lower temperature
limit of 45K thermal emission always empties all states at
energies lower than E_λ = 0.08 eV.

Fig. 19: Effect of stray light for different capacitances. A large
amplitude and a strong relaxation when the light was turned off
is clearly visible.

After this observation, we carefully checked all the filters
for leakage. The three filters used (5μm, 6μm, and 7,5μm)
did not show large relaxations when the light was turned off.
The filter at 10μm showed a relaxation. It was therefore
rejected from the measurements. The filter with center wavelength
at 15μm could not be used because with the lower temperature
limit of 45K thermal emission always empties all states at
energies lower than E_λ = 0.08 eV.

Al-Gate Electrodes

In initial experiments samples with Al-gate electrodes
(e.g. HU10/II in Fig 19) have been used. These samples
were illuminated between the gate electrodes so that light
can reach the interface under the electrode only by multiple
reflection and scattering. The photon flux in this case is
smaller than by direct illumination with a transparent electrode.
Because of the small absorption cross-section transients
cannot be measured.

Even for the transparent electrodes, the photon flux was
not sufficient. An infrared source of higher power than the
globar is needed for more accurate measurements.

Stability

The small amplitude of the transients (10^8cm^{-2} levels have
to be resolved (Fig. 14)) and the slow time constants
(observation times of several hours are necessary) impose
serious stability requirements on the apparatus. A drift
in the dc bias voltage contributes directly to the transient.
The stability must be better than 1mV/hour.

A temperature stability of 2K was usually satisfactory.
Only in the region where carrier freeze-out occurs and the
capacitance measurement is affected by series resistances
a strong effect of the temperature fluctuation is observed.
The 0.5K stability of the cryostat used was sufficient.

VII Conclusions

We have shown that photoexcitation of MOS interface states
near the conduction band edge at 0.10 eV to 0.24 eV by infrared
light in the wavelength range 5μm to 7.5μm is possible.
The density of interface states and optical absorption cross-
sections could be determined. In the well-behaved sample B
the same density of states as in electrical measurements
(CC-DLTS and quasistatic technique) is observed. The optical
cross-section at these energies and wavelengths is found to be
of the order of 3×10^{-19}cm². The absorption cross-section
increases with photon energy and decreases with increasing
energy depth for the interface states for a fixed wavelength.

The sample A having a high density of interface states shows
the same qualitative behavior for the optical properties.
Irregularities were observed in the density of states which
seemed to be temperature dependent.

The expected independence of the optical measurement of
potential fluctuations could be confirmed for the well-
behaved sample B. In sample A, an influence of potential
fluctuations was observed, but the measurement was still possible.

A decision with respect to interpretation of interface states
by various models is too early with the limited amount of data
taken. The result of sample A shows very complicated behavior
which is not yet understood. However, the small absorption cross-
section observed and the variation with wavelength and energy
do not contradict the model, which we suggested in an ealier
publication. In this model, interface states are assumed to
be located in SiO_2. The continuous distribution is explained

by a relation of the energy position to the distance from
the interface. For such states we expect low values of the
absorption cross-section and a further decrease at long
wavelength because the transfer from SiO_2 to the Si is less
probable for small excitation energies. Further experiments
should be based on samples with an intermediate interface
state density (between sample A and B) to improve the
accuracy and to avoid the problems met in sample A having too
high a density.

The temperature dependence of the interface state observed
in sample A is a new effect which we do not understand at
present. It may be related to a trap level the energy of which
is affected directly or indirectly through strain introduced
by the temperature. We will pursue this effect further.

VIII   Literature

/1/   A. Goetzberger, E. Klausmann, M. Schulz
        Interface States on Semiconductor / Insulator Surfaces
        CRC Critical Review in Solid State Sciences 1976

/2/   E. Klausmann, A. Goetzberger
        Dynamic Properties of Interface States in MOS-Structures
        Final Technical Report, Freiburg, 1980

/3/   M. Schulz, E. Klausmann
        Transient Capacitance Measurement of Interface States
        on the Intentionally Contaminated $Si-SiO_2$-Interface
        Appl.Phys. 18, 169-175, 1979

/4/   E. Klausmann
        The Evaluation of Transient Capacitance Measurements on
        MOS Interfaces
        Inst. Phys. Conf. Ser. No. 50, p. 97, 1979

/5/   M. Schulz
        MOS Interface States
        Inst. Phys. Conf.Ser. No. 50, p.87, 1979

/6/   D.W. Greve
        Photoionisation of States in MOS Devices
        Dissertation, Lehigh University, Bethlehem, 1979

/7/   D.W. Greve, W.E. Dahlke
        Photoemission from Interface States in MOS Structures
        Inst. Phys. Conf.Ser. No. 50, p 107, 1979

/8/   R.F. Pierret, B.B. Roesner
       Photoemission from Surface Centers
       Appl. Phys. Letters, Vol. 24, No. 8, 1974

/9/   K. Schroder, R.N.Thomas, J.C. Schwartz
       Free Carrier Absorption in Silicon
       IEEE Trans. on Electr. Dev., Vol.ED 25, No.2, 1978

/10/   W. Frick, H. Rabethge
       Photoemission aus Grenzflächenzuständen an Si-MOS-Strukturen
       Verhandlungen der Dt.Physikal. Gesellschaft 3/1980, HL 158

/11/   W. Frick, H. Rabethge
       priv. communication